

# Polarization of Intraprotein Hydrogen Bond Is Critical to Thermal Stability of Short Helix

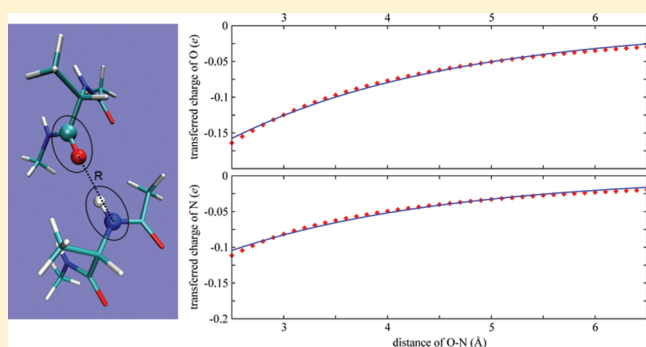
Ya Gao,<sup>†</sup> Xiaoliang Lu,<sup>†</sup> Li L. Duan,<sup>‡</sup> John Z. H. Zhang,<sup>\*,†,§</sup> and Ye Mei<sup>\*,†</sup>

<sup>†</sup>State Key Laboratory of Precision Spectroscopy and Department of Physics, Institute of Theoretical and Computational Science, East China Normal University, Shanghai 200062, China

<sup>‡</sup>College of Physics and Electronics, Shandong Normal University, Jinan 250014 Shandong, China

<sup>§</sup>Department of Chemistry, New York University, New York, New York 10003, United States

**ABSTRACT:** Simulation result for protein folding/unfolding is highly dependent on the accuracy of the force field employed. Even for the simplest structure of protein such as a short helix, simulations using the existing force fields often fail to produce the correct structural/thermodynamic properties of the protein. Recent research indicated that lack of polarization is at least partially responsible for the failure to successfully fold a short helix. In this work, we develop a simple formula-based atomic charge polarization model for intraprotein (backbone) hydrogen bonding based on the existing AMBER force field to study the thermal stability of a short helix (2I9M) by replica exchange molecular dynamics simulation. By comparison of the simulation results with those obtained by employing the standard AMBER03 force field, the formula-based atomic charge polarization model gave the helix melting curve in close agreement with the NMR experiment. However, in simulations using the standard AMBER force field, the helix was thermally unstable at the temperature of the NMR experiment, with a melting temperature almost below the freezing point. The difference in observed thermal stability from these two simulations is the effect of backbone intraprotein polarization, which was included in the formula-based atomic charge polarization model. The polarization of backbone hydrogen bonding thus plays a critical role in the thermal stability of helix or more general protein structures.



## INTRODUCTION

How protein folds to its precisely defined structure has been one of the most challenging problems for contemporary physical chemistry research, pharmaceutical science, and protein engineering. Understanding the mechanism of folding is important from both experimental and theoretical perspectives. The stable structure of protein has a minimum free energy (mostly global minimum) that is reached as a balance of all types of physical interactions within the protein and between the protein and its environment. Because these interactions are highly specific, the accurate prediction of the stable structure of protein is extremely difficult. From a theoretical perspective, the challenge is a grand one because the free energy difference between the folded and unfolded (or misfolded) states are typically just a few kcal/mol. Thus the prediction of the protein structure is highly dependent on the quality of the force field used. To correctly differentiate the folded structure from misfolded ones, the force field used in theoretical prediction has to be as reliable as possible. Unfortunately, the currently available force fields have deficiencies that make the theoretical prediction of the protein structure extremely difficult.<sup>1</sup>

An important property is the protein thermal stability, which has been only partially understood despite its significant

importance in both academic and industrial arenas. Understanding the physical principles of thermal stability will aid in our understanding of protein folding and interaction mechanisms. Among many factors that are important to protein stability, the number of hydrogen bonds is found to correlate highly with the thermal stability of a protein (both intraprotein and protein-water hydrogen bonds).<sup>2</sup> Hydrogen bonds are perhaps the most important structural element of protein. They are the dominant feature in protein secondary structures of  $\alpha$  helices and  $\beta$  sheets. Recent theoretical studies demonstrated that the strength of hydrogen bonds from simulations under standard nonpolarizable force fields are underestimated due to the lack of polarization effect.<sup>3–10</sup> Thus it is important to examine how the polarization of protein hydrogen bonds affects the thermal stability of protein. In previous works,<sup>11</sup> polarization of the backbone hydrogen bonding is found to be critical to the successful folding of small helices. In these works, the polarization of hydrogen bonds is included in the dynamics simulation by performing on-the-fly

**Received:** September 16, 2011

**Revised:** November 16, 2011

**Published:** November 29, 2011

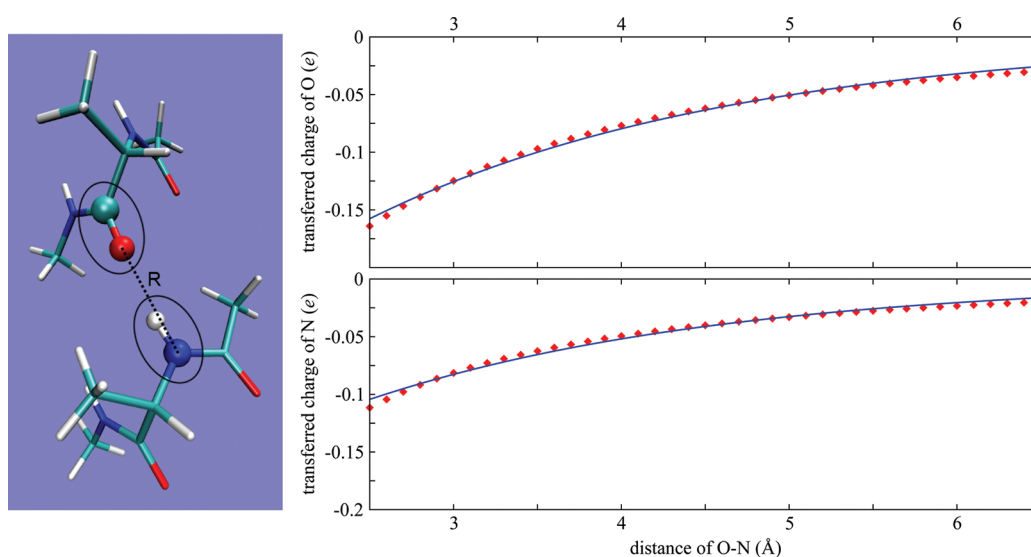


**Figure 1.** Left: model system used in fitting the atomic charge polarization as a function of donor–acceptor distance in hydrogen bond pair. The charge transfer is only allowed between N and H, and between C and O as depicted in the ellipses. Right: amount of charge transfer as a function of donor–acceptor distance for atoms O (top) and N (bottom).

quantum calculation to generate dynamically updated atomic charges in the standard MD simulation of folding.<sup>11,12</sup>

However, on-the-fly quantum calculation is computationally expensive, in which quantum mechanical calculation must be periodically carried out to obtain new atomic charges for residues with changing hydrogen bonds. It is thus desirable to employ a simpler but effective method to include polarization of hydrogen bond for efficient protein simulation. In this work, we propose a new polarization model for hydrogen bond based on the analytical fit of atomic charges to precomputed hydrogen bond residue pairs. This simpler analytical model is computationally efficient and we employ it in replica exchange molecular dynamics (REMD) approach to studying folding of the helix.

This paper is organized as follows. In the next section, we describe the polarization model for hydrogen bond and the details of folding simulations of the helix 2I9M. Then the folding results from utilizing both the standard AMBER and the polarized atomic charges are discussed. Finally, we give a summary of the present work.

## METHODOLOGY

When a hydrogen bond (such as the backbone CO–HN hydrogen bond between the two amino acids) is formed, the electron density distribution will be distorted due to mutual polarization between the donor and acceptor of the hydrogen bond. This polarization effect lowers the electrostatic interaction energy between the donor and acceptor and makes the hydrogen bond a bit stronger. This added strength in hydrogen bonding due to polarization was shown to be critical to stabilize the folding of helix.<sup>11</sup> However, under standard nonpolarizable force field such as AMBER03, the atomic charges are fixed and therefore no polarization effect is included in the dynamics simulation. There currently exists a number of polarizable models for proteins<sup>13–15</sup> for MD simulation. But these models at present are still too complicated to apply and their accuracy still needs to be further validated. Here we propose a simple polarization model specifically for hydrogen bond–backbone hydrogen bonding in particular.

We used a pair of dialanine in  $\alpha$ -helical structure as a model system for backbone hydrogen bonding. Atomic charges of the acceptor and donor of the hydrogen bond of the dialanine are fitted to electrostatic potential generated from quantum chemistry calculation using the RESP scheme.<sup>16–18</sup> By varying the donor–acceptor distance but keeping the other geometries of the dialanine fixed, we obtained RESP charges for the donors and acceptors at discrete points along the bond length (shown as the dashed line in Figure 1a) between 2.5 Å and 6.5 Å. The calculated amount of charge deviations from their asymptotic values for atoms N and O are shown in Figure 1b (red diamonds), both of which can be fitted to a single-exponential function (blue curves). In this approach, no charge transfer between residues is allowed and only the atomic charges of the N, H, C, and O atoms in the hydrogen bond are varied. Thus, the amount of transferred charge for H and C atoms is exactly the negative of that for N and O atoms, respectively. The fitted functional forms are

$$\Delta q_N = -0.843 \times \exp[-0.455(R + 1.18)] \quad (1)$$

and

$$\Delta q_O = -0.250 \times \exp[-0.466(R - 0.623)] \quad (2)$$

for N and O atoms, respectively, in which  $R$  is the donor–acceptor distance in angstroms. As shown in Figure 1, the total amount of charge transfer is not remarkable, but only about 0.1e and 0.13e for N and O atoms at the normal bond length ( $\sim 3$  Å). In our current method, only charges of the N, H, C, and O atoms of the donors and acceptors are functions of the hydrogen bond distance whereas atomic charges of other atoms are assigned fixed AMBER charges. When the two ALAs are infinitely separated, the residues are given the corresponding AMBER charges. In the charge fitting procedure, mutual polarization was included. Specifically, in the calculation of one residue, the other was taken as background charges centered at atomic positions. Iteration was performed until convergence is reached. We also found that the charge variation with the hydrogen bond angle is quite small. Thus the charge variation can largely be determined by hydrogen bond length alone. We believe this is a good approximation. And

we only considered the main chain hydrogen bonds. Other types of hydrogen bonds like those between main chain/side chain atoms or side chain/side chain hydrogen bonds, as well as salt bridges, also have strong electrostatic polarization effect. They may be taken into consideration by refined versions of this approach. Quantum mechanical calculations were performed at HF/6-31G\* level using the Gaussian09 package.<sup>19</sup>

## RESULTS AND DISCUSSION

We employed this polarizable hydrogen bond (PHB) model to study the thermal stability of a short helix 2I9M.<sup>20</sup> The 2I9M is a “de novo” designed 17-residue peptide whose native state is a helix. The structure of 2I9M was determined by NMR experiment at 283 K and pH = 5.0. To study the thermal stability, REMD simulation is carried out with an implicit GB solvation model. REMD are now routinely applied to studying folding of small proteins. In REMD simulation, high temperature replicas can easily surmount the energy barrier and can explore the phase space more efficiently than in the standard molecular dynamics at room temperature. It has been shown that REMD is about 1 order of magnitude more efficient than the direct molecular dynamics simulation of folding.<sup>21</sup> Kim et al.<sup>22</sup> carried out a 60 ns per replica REMD simulation study of 2I9M with a modified force field (param99MOD/GBSA) with a total of 14 replicas. Their lowest free energy structure agreed with the NMR structure. In the present study, we carried out REMD simulations with 12 replications (temperatures 267, 283, 300, 328, 353, 380, 409, 439, 471, 506, 542, and 577 K). Two sets of MD simulations were performed here using, respectively, the standard AMBER03 and the present formula-based PHB model. In this PHB model, only atomic charges of donors and acceptors in hydrogen bonds are different whereas other force field parameters were taken from the AMBER03 force field.

The starting conformation was a linear structure generated using LEaP module in AmberTools and was relaxed until convergence was reached. The relaxed structure was heated to its target temperature for each replica in 100 ps. Solvation effect was modeled using the generalized Born (GB) model developed by Onufriev, Bashford, and Case.<sup>23</sup> The salt concentration was set to 0.2 M and the integration time step was 1 fs. All bonds with hydrogen atoms were fixed using SHAKE algorithm.<sup>24</sup> Non-bonded interaction was counted without any truncation. Temperature was regulated using Langevin dynamics with the collision frequency of 1 ps<sup>-1</sup>. Swaps were attempted every 0.25 ps and MD simulations were extended to 120 ns for each replica, and snapshots were saved every 0.25 ps. The MD simulations were carried out using AMBER 10 package with some home-made modifications.<sup>25</sup> Free energy was calculated by Weighted Histogram Analysis Method (WHAM)<sup>26,27</sup> using density of state estimated by

$$\Omega_{mk} = \frac{H_{mk}}{\sum_{l=1}^L N_{kl} \Delta U \exp[f_l - \beta_l U_m]}$$

When the formula-based polarization model was used, hydrogen bonds were detected using the Simulaid program<sup>28</sup> every 0.25 ps. More frequent checking can increase the accuracy but will reduce the efficiency of simulation.

The folded state is defined as having rmsd from NMR structure below 2 Å in our study. The populations of the folded

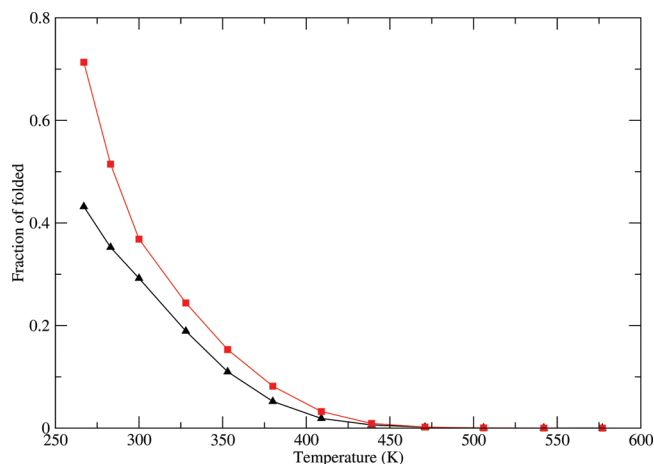


**Figure 2.** Fraction of folded structure defined by root-mean-square deviation from the NMR structure below 2 Å as a function of temperature in the simulations utilizing AMBER03 charge (black) and PHB charge (red).

structure in two REMD simulations show a clear difference, as shown in Figure 2. At the lowest temperature (267 K), the percentage of folded structure in AMBER03 force field was nearly 30% lower than that in the PHB model. At the temperature of NMR experiment (283 K), the fraction of folded structure in AMBER03 force field is about 35% whereas that in the PHB model is over 50%. The melting curves from both the AMBER03 force and PHB model are plotted in Figure 2. Comparison of the melting curves shows that the melting temperature in the standard AMBER03 force field is too low (below 267 K), well below the NMR experimental temperature of 283 K. This means that under standard AMBER03 force field, the 2I9M is thermally unstable. In a previous study, the direct MD simulation failed to fold 2I9M into the native structure under the standard AMBER03 force field.<sup>11</sup> The present REMD simulation shows that 2I9M is thermally unstable at room temperature and the result is highly consistent with the direct simulation study of ref 11. This is an important observation because the AMBER03 force field is known to favor helix structures.

The melting temperature is defined as the temperature at which the free energy of the native and unfolded states are equal. Thus the folded and unfolded structures should be equally populated (50% each). Using this definition, the melting temperature under the AMBER03 force field is even below 263 K, well below the NMR temperature of 283 K. This is obviously inconsistent with the experimental observation. The criterion of rmsd ≤ 2 Å chosen to define the folded state is a reasonable choice as will be seen later from free energy analysis. The REMD result under the PHB model (based on the AMBER03 force field) shows a thermally stable 2I9M. The melting curve in Figure 2 gives a melting temperature of about 286 K, above the NMR temperature at 283 K. This result shows that hydrogen bond polarization is critical to the thermal stability of the helical structure of 2I9M.

The distribution of the peptide structure from the REMD simulation in the REMD space is determined by the free energy distribution. Figure 3 plots the free energy changes along the rmsd at 267, 283, and 300 K using both the AMBER03 and PHB model. We first examine the free energy under AMBER03 charge. At 267 K (top figure), the free energy curve has a global



minimum at rmsd around 1.6 Å and also a local minimum at a rmsd value around 4 Å (unfolded state). We note that the free energy at this local minimum is only 0.5 kcal/mol higher than at the global minimum. Thus, there were comparable distributions of structures at these two geometries. For comparison, the free energy curve under the PHB model displays two nearly degenerate minima at rmsd near 1.25 and 1.6 Å, both represent folded structures. In fact, the free energy is essentially flat in the region between these two minima. The free energy curve shows a very shallow local minimum at rmsd = 3.5 Å, which is about 1 kcal/mol higher than the global minimum. This free energy analysis explains why the helix is thermally more stable under the PHB model.

At increased temperatures, the free energy curve becomes flatter and the minimum at 1.25 Å gradually disappears but the minimum at 1.6 Å remains, as shown in the middle and bottom figures of Figure 3. By comparing the free energy curves at 283 and 300 K with those at 267 K, we observe that the free energy difference between the folded and unfolded states gradually diminished.

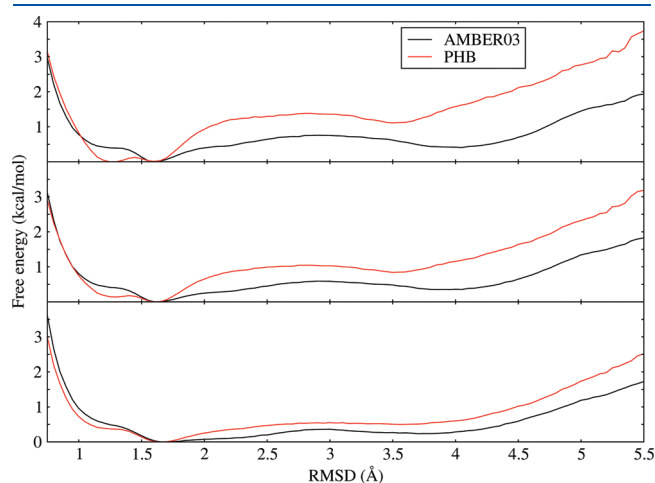


**Figure 3.** Free energy curves as a function of the rmsd from the NMR structure in simulation utilizing AMBER03 charge (black) and PHB charge (red) at (top) 267 K, (middle) 283 K, and (bottom) 300 K.

The difference of free energy between AMBER03 charge and PHB model is also reduced with the increasing temperature.

We next plot the free energy landscapes in 2D space spanned by mass-weighted root-mean-square deviation (rmsd) from the NMR structure and radius of gyration ( $R_g$ ) at 283 K. The  $R_g$  calculated from the experimental structure, excluding the terminal residues, is 7.14 Å. The free energy landscapes obtained from both AMBER03 charge and the PHB model shown in Figure 4. In both simulations, the native structure was identified with rmsd below 2 Å and  $R_g$  near the vicinity of the experimental value. In the simulation using AMBER03 charge, a misfolded state with only partially folded structure near an rmsd value of 4 Å, as shown in Figure 4 (left), was also detected with the free energy just a bit higher than the native structure. The free energy contour shows a large flat area with rmsd below 5 Å and  $R_g$  between 7 and 8 Å. The majority of the population lies within this area with both folded and unfolded states (rmsd >2). This is also seen in Figure 2 in which the fraction of the folded structure is only 36% at 283 K. Although the combination of AMBER03 force field and IGB5 is believed to bias the helical structure, they still failed to correctly fold the helix structure of this short peptide. In a previous study, this peptide did not fold to its native structure in the standard molecular dynamics simulation under the same force field and solvation model.<sup>11</sup>

For comparison, the free energy landscape in the PHB model near the folded structure is steeper than that in the AMBER03 charge and therefore the native structure is energetically more stable than the unfolded ones, as shown in Figure 4 (right). Specifically, the native structure is about 1.0 kcal/mol more stable than unfolded ones at the temperature of the NMR experiment. From the analysis of both the one-dimensional free energy profile and 2D free energy landscape, we can conclude that starting from the extended initial structure (rmsd >5,  $R_g$  > 11), the peptide underwent a rather straightforward downhill free energy path without encountering any free energy barrier below the melting temperature in the PHB model. In contrast, under the standard AMBER03 charge, there is a local minimum corresponding to partially folded states of the peptide along the free energy path to the native state.

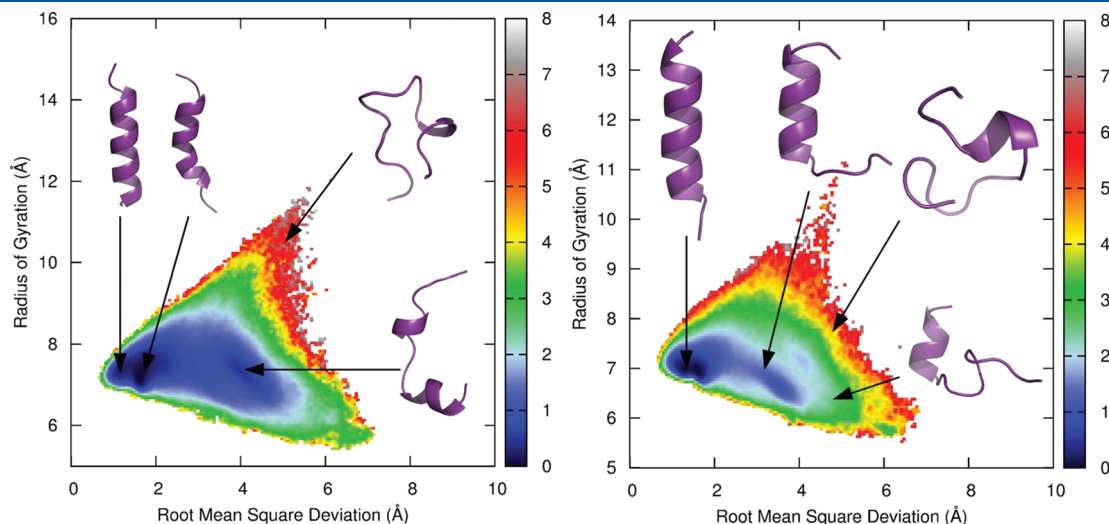


**Figure 4.** Fitted free energy landscape in the 2D space of root-mean-square deviation from the NMR structure and radius of gyration from the trajectory at 283 K (left) utilizing AMBER03 charge and (right) the PHB model.

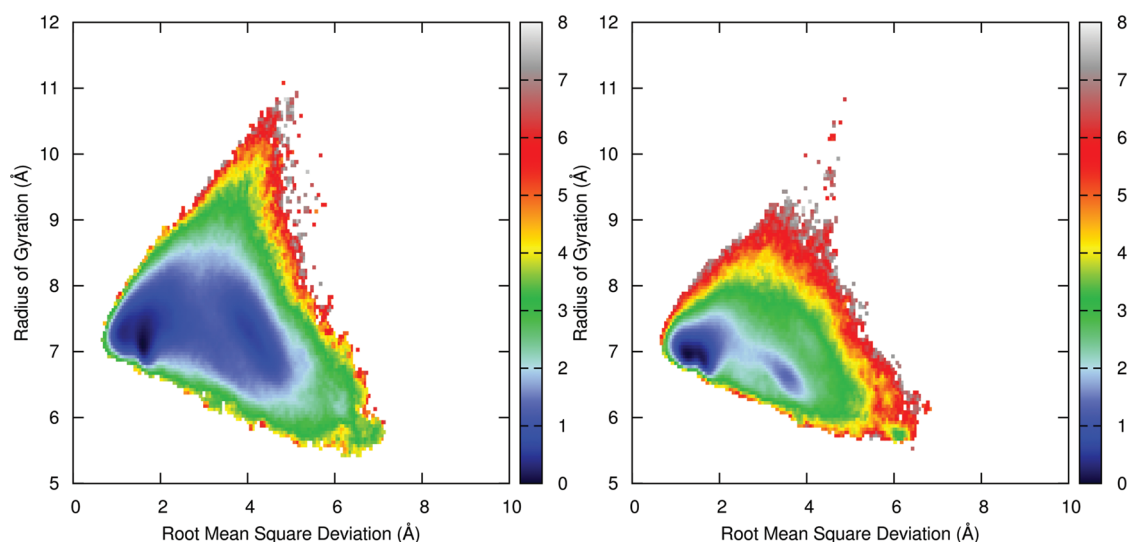


Figure 5. Same as Figure 4, except the temperature is 273 K.

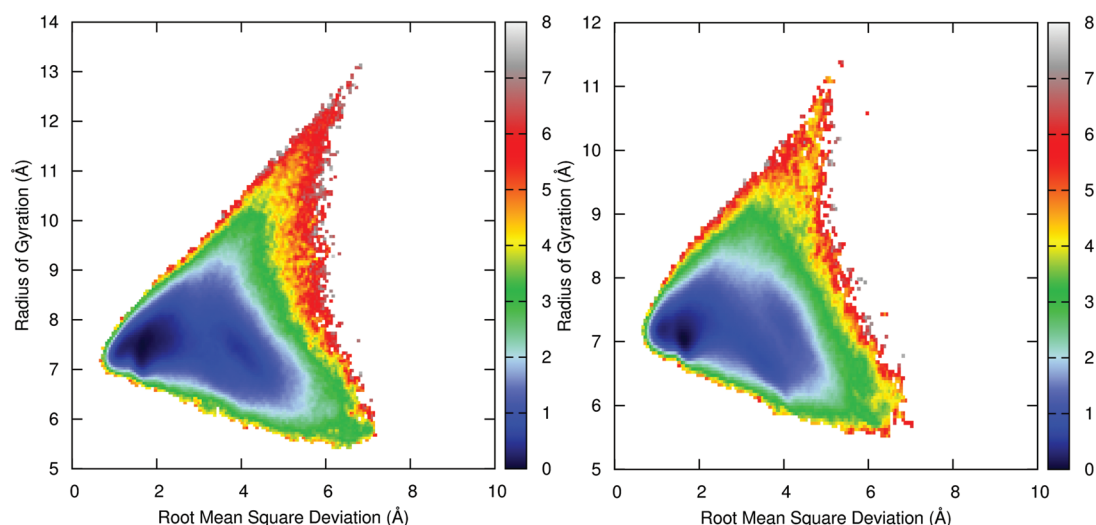
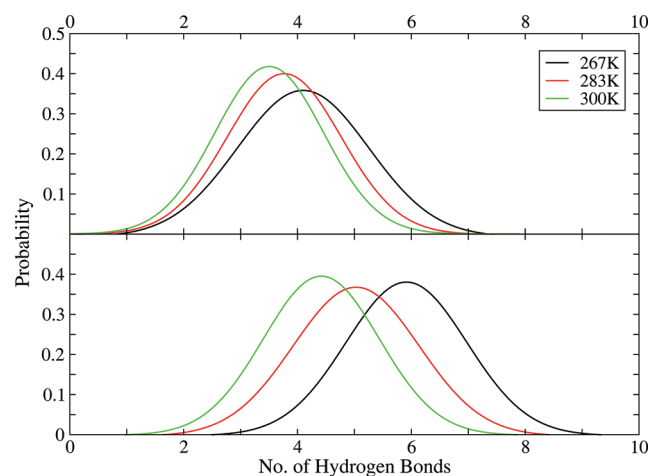


Figure 6. Same as Figure 4, except the temperature is 300 K.

Comparison of the free energy landscapes at different temperatures may help to illustrate the thermal stability of the protein. We plotted the 2D free energy landscapes at both the freezing point (273 K) and room temperature (300 K) in Figures 5 and 6, respectively. Lowering the temperature to 273 K increases the free energy gap between the folded and the unfolded states, and raising the temperature to 300 K achieves the opposite effect. For results under AMBER03 charge at 273 K, we noticed a clear free energy barrier separating the folded state from the unfolded state and both states have sizable populations. At 300 K, the free energy landscape is essentially flat, indicating the protein is already melted. For results under the PHB model at 273 K, the native structure was much steeper than that at 283 K, and the unfolded decoy structure was much less populated. At 300 K (higher than the predicted melting temperature), the free energy landscape is more smeared, showing the status of melting. The result of these 2D free energy landscapes is highly consistent with the 1D free energy curves discussed above.

The present study, together with the previous study on direct folding of 219M,<sup>11,12</sup> points to the importance of polarization of backbone hydrogen bonding to the helix formation and the thermal stability of the helix. This claim is consistent with the observed effect of hydrogen bond cooperativity.<sup>29–32</sup> The hydrogen bonds in the trajectories were identified using *Simulaid*,<sup>28</sup> and we counted the hydrogen bonds using a sigmoidal function of the donor–acceptor distance  $d$  as  $f_{\text{HB}}(d) = 1/(1 + (x/2.6)^6)$  related to the strength of hydrogen bonds. In Figure 7, we plotted the distribution of the number of hydrogen bonds (divided by 0.58, which is the largest value of  $f_{\text{HB}}$ ) at 267, 283 and 300 K in both REMD MD simulations. It shows that the peak shifts from 3.8 under the AMBER03 charge to 5.0 under the PHB model at 283 K, indicating that hydrogen bonds were strengthened when the polarization effect was included. Decreasing the temperature to 267 K, the difference between the AMBER03 charge and PHB model becomes more remarkable, whereas increasing the temperature to 300 K does the opposite.



**Figure 7.** Distribution of native hydrogen bonds population in 267, 283 and 300 K trajectories utilizing the AMBER03 charge (top) and PHB model (bottom).

## CONCLUSION

In this work, we proposed a formula-based polarizable hydrogen bond model that can be implemented in REMD as well as standard MD simulation studies of proteins. REMD simulation using the PHB model with GB solvation has been applied to studying the folding and the thermal stability of a short helical peptide 2I9M. The melting temperature is about 286 K, just above the NMR experimental temperature of 283 K. The folding is a direct downhill motion without encountering appreciable metastable states or decoy states. For comparison, REMD simulation using the AMBER03 charge gives a melting temperature well below the freezing point (273 K), indicating that the peptide is not stable at the temperature of NMR experiment. This is clearly in violation of the experimental observation. Free energy landscape analysis shows that the folding under AMBER03 charge went through a decoy structure with rmsd at about 4 Å. Further improvement of this method is also available. More sophisticated extension of the current PHB model that can accurately treat the polarization of other general types of hydrogen bonds can be envisioned. Conformation-dependent atomic charges and charge transfer can also be implemented to differentiate the secondary structure as has been done before.<sup>33</sup> Also the dependence on force fields<sup>34</sup> and hydrogen bond cooperativity will also be investigated in the future. We believe that this formula-based PHB model is a promising method for computational study of proteins or other biopolymers.

## AUTHOR INFORMATION

### Corresponding Author

\*E-mail: J.Z.H.Z., john.zhang@nyu.edu; Y.M., ymei@phy.ecnu.edu.cn.

## ACKNOWLEDGMENT

This work is supported by the National Science Foundation of China (Grant No. 20803034 and 20933002), Shanghai Pujiang program (09PJ1404000), Shanghai Rising-Star program and Innovation Fund of East China Normal University. We also thank the High Performance Computer Center of East China Normal University and Shanghai Supercomputer Center for CPU time support.

## REFERENCES

- (1) Freddolino, P. L.; Park, S.; Roux, B.; Schulten, K. *Biophys. J.* **2009**, *96*, 3772–3780.
- (2) Vogt, G.; Woell, S.; Argos, P. *J. Mol. Biol.* **1997**, *269*, 631–643.
- (3) Ji, C. G.; Zhang, J. Z. H. *J. Am. Chem. Soc.* **2008**, *130*, 17129–17133.
- (4) Duan, L. L.; Mei, Y.; Zhang, Q. G.; Zhang, J. Z. H. *J. Chem. Phys.* **2009**, *130*, 115102.
- (5) Lu, Y. P.; Mei, Y.; Zhang, J. Z. H.; Zhang, D. W. *J. Chem. Phys.* **2010**, *132*, 131101.
- (6) Wei, C. Y.; Mei, Y.; Zhang, D. W. *Chem. Phys. Lett.* **2010**, *495*, 121–124.
- (7) Xu, Z. J.; Mei, Y.; Duan, L. L.; Zhang, D. W. *Chem. Phys. Lett.* **2010**, *495*, 151–154.
- (8) Tong, Y.; Ji, C. G.; Mei, Y.; Zhang, J. Z. H. *J. Am. Chem. Soc.* **2009**, *131*, 8636–8641.
- (9) Ji, C.; Zhang, J. Z. H. *J. Phys. Chem. B* **2009**, *113*, 13898–13900.
- (10) Tong, Y.; Mei, Y.; Li, Y. L.; Ji, C. G.; Zhang, J. Z. H. *J. Am. Chem. Soc.* **2010**, *132*, 5137–5142.
- (11) Duan, L. L.; Mei, Y.; Zhang, D. W.; Zhang, Q. G.; Zhang, J. Z. H. *J. Am. Chem. Soc.* **2010**, *132*, 11159–11164.
- (12) Wei, C. Y.; Tung, T.; Yip, Y. M.; Mei, Y.; Zhang, D. W. *J. Chem. Phys.* **2011**, *134*, 171101.
- (13) Banks, J. L.; Kaminski, G. A.; Zhou, R. H.; Mainz, D. T.; Berne, B. J.; Friesner, R. A. *J. Chem. Phys.* **1999**, *110*, 741–754.
- (14) Lamoureux, G.; MacKerell, A. D., Jr.; Roux, B. *J. Chem. Phys.* **2003**, *119*, 5185–5197.
- (15) Warshel, A.; Levitt, M. *J. Mol. Biol.* **1976**, *103*, 227–249.
- (16) Bayly, C. I.; Cieplak, P.; Cornell, W.; Kollman, P. A. *J. Phys. Chem.* **1993**, *97*, 10269–10280.
- (17) Cornell, W. D.; Cieplak, P.; Bayly, C. I.; Kollman, P. A. *J. Am. Chem. Soc.* **1993**, *115*, 9620–9631.
- (18) Cieplak, P.; Cornell, W. D.; Bayly, C.; Kollman, P. A. *J. Comput. Chem.* **1995**, *16*, 1357–1377.
- (19) Frisch, M. J.; Trucks, G. W.; Schlegel, H. B.; Scuseria, G. E.; Robb, M. A.; Cheeseman, J. R.; Scalmani, G.; Barone, V.; Mennucci, B.; Petersson, G. A. et al. *Gaussian 09*, Revision B.01; Gaussian, Inc.: Wallingford, CT, 2010.
- (20) Pantoja-Uceda, D.; Pastor, M. T.; Salgado, J.; Pineda-Lucena, A.; Perez-Paya, E. *J. Pept. Sci.* **2008**, *14*, 845–854.
- (21) Nymeyer, H. *J. Chem. Theory Comput.* **2008**, *4*, 626–636.
- (22) Kim, E.; Jang, S.; Pak, Y. *J. Chem. Phys.* **2008**, *128*, 175104.
- (23) Onufriev, A.; Bashford, D.; Case, D. A. *Proteins* **2004**, *55*, 383–394.
- (24) Ryckaert, J.-P.; Ciccotti, G.; Berendsen, H. J. C. *J. Comput. Phys.* **1977**, *23*, 327–341.
- (25) Case, D. A.; Darden, T. A.; Cheatham, T. E., III; Simmerling, C. L.; Wang, J.; Duke, R. E.; Luo, R.; Crowley, R.; Walker, R. C.; Zhang, W. et al. *AMBER 10*; University of California: San Francisco, 2008.
- (26) Kumar, S.; Rosenberg, J. M.; Bouzida, D.; Swendsen, R. H.; Kollman, P. A. *J. Comput. Chem.* **1992**, *13*, 1011–1021.
- (27) Chodera, J. D.; Swope, W. C.; Pitera, J. W.; Seok, C.; Dill, K. A. *J. Chem. Theory Comput.* **2007**, *3*, 26–41.
- (28) Mezei, M. *J. Comput. Chem.* **2010**, *31*, 2658–2668.
- (29) Wu, Y.-D.; Zhao, Y.-L. *J. Am. Chem. Soc.* **2001**, *123*, 5313–5319.
- (30) Viswanathan, R.; Asensio, A.; Dannenberg, J. J. *J. Phys. Chem. A* **2004**, *108*, 9205–9212.
- (31) Kobko, N.; Dannenberg, J. J. *J. Phys. Chem. A* **2003**, *107*, 10389–10395.
- (32) Ireta, J.; Neugebauer, J.; Scheffler, M.; Rojo, A.; Galvan, M. *J. Phys. Chem. B* **2003**, *107*, 1432–1437.
- (33) Jorgensen, W. L.; Gao, J. *J. Am. Chem. Soc.* **1988**, *110*, 4212–4216.
- (34) Hegefeld, W. A.; Chen, S.-E.; DeLeon, K. Y.; Kuczera, K.; Jas, G. S. *J. Phys. Chem. A* **2010**, *114*, 12391–12402.